Instrument Overview

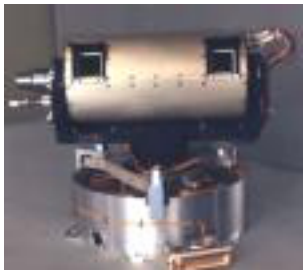

The Imager for Mars Pathfinder or IMP is a stereo imaging system with color capability provided by twenty-four selectable filters for the two camera channels. It is derived from the descent imager/spectral radiometer (DISR) instrument aboard the Cassini Huygens probe.

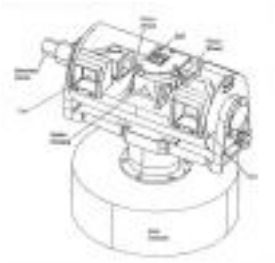

Scientific Objectives

The IMP camera was designed to study martian geological processes and surface-atmosphere interactions similar to what was observed at the Viking landing sites. Through the use of panoramic stereo images taken at various times of the day, it was also used to observe the general landscape, surface slopes, and the distribution of rocks. Changes in the scene over the lifetime of the mission, possibly attributable to the actions of frost, dust or sand deposition, erosion or other surface-atmosphere interactions, were monitored. A greater understanding of the surface and near-surface soil properties was sought. This was to be obtained partly with data acquired by the Rover and APXS and partly by IMP imaging of Rover wheel tracks, holes dug by the Rover wheels, and any surface disruptions caused by airbag bounces or retractions.

An investigation was made of atmospheric aerosols and water vapor. This included the determination of the aerosol optical depth as a function of wavelength above the landing site, the size and density distribution of the aerosols, a characterization of the shape of the aerosol particles, the vertical distribution of the aerosols, and the imaginary refractive index of the particles.

The IMP experiment also included a magnetic properties investigation. A set of magnets of differing field strengths were mounted to a plate and attached to the lander. Images taken over the duration of the landed mission were used to determine the accumulation of magnetic species in the wind-blown dust. Multispectral images of these accumulations were used to differentiate among the several proposed mineral compositions.

The IMP investigation included the observation of wind direction and velocity using wind socks mounted on the ASI/MET mast.

Subsystems

The IMP consists of three physical subassemblies: (1) camera head (with stereo optics, filter wheel, CCD and pre-amp, mechanisms and stepper motors); (2)

extensible mast with electronic cabling; and (3) two plug-in electronics cards (CCD data card and power supply / motor drive card) which plug into slots in the lander's Integrated Electronics Module.

The major components of the camera head and electronics cards are described in greater detail below.

The extensible mast was built by AEC Able Corp, and is a continuous longeron, open-lattice type used for magnetometers. It was held in its stowed position during cruise by a pyro-activated pin puller. Upon deployment, the camera system, mounted at the top of the mast, sprung up to a height of 62 cm above its stowed position, or roughly .9 meters above the surface of Mars.

Detectors

Azimuth and elevation drives for the camera head are provided by stepper motors with gear heads, providing a field of regard of ±178° in azimuth and +83° to -72° in elevation, relative to lander coordinates.

IMP Mechanical Characteristics

Stereo separation	15.0 cm
Toe-in	12.5 mrad (left); -24.5 mrad (right)
AZ/EL step size	0.553°, 1° hysteresis (backlash)
Repeatability	< 5 mrad, when approaching from the same direction
Step speed	10 steps per second
Pointing range	360° azimuth, +90° to -67° elevation
Data compression	1.3:1 lossless up to 24:1 lossy (JPEG) (higher compression ratios achieved using pixel blocking)

The focal plane of the IMP consists of a CCD mounted at the foci of two optical paths where it is bonded to a small printed wiring board, which in turn is attached by a short flex cable to the preamplifier board. The CCD is a front-illuminated frame transfer array with 23 micrometer square pixels. Its image section is divided into two square frames, one for each half of the stereo FOV's. Each has 256 x 256 active elements. A 256 x 512 storage section (identical to the imaging section) is located under a metal mask. The IMP focal plane and electronics are nearly identical copies of the comparable subsystem employed in the Huygens Probe Descent Imaging Spectroradiometer (DISR), using the Loral 512 x 512 CCD. The entire CCD subsystem is provided by the Max Planck Institute for Aeronomy.

CCD Specifications

Readout noise	15 electrons

Full well	125,000 electrons
Readout time	2 sec. for full array; 1 sec. for left eye only
Exposure time	0 - 32.7675 seconds; step size is 0.5 milliseconds
Spectral range	440 - 1000 nm
Gain	30 electrons/pixel
ADC	12 bits/pixel
Frame transfer	0.5 milliseconds (no mechanical shutter)
SNR	<= 350
Pixel size	23 x 17 micrometers; 6 micrometers for an antiblooming channel

Optics

The stereoscopic imager includes two imaging triplets, two fold mirrors separated by 150 mm for stereo viewing, two 12-space filter wheels (one in each path), and a fold prism to place the images side-by-side on the CCD focal plane. Fused silica windows at each path entrance prevent dust intrusion. The optical triplets are an f/10 design, stopped down to f/18 with 23 mm effective focal lengths and a 14.4° field of view. The pixel instantaneous field of view is one milliradian. There are a total of 24 filters (twelve on each filter wheel) divided into the following categories: four stereo geology channels, eleven monoscopic geology channels, eight monoscopic channels for solar and atmospheric studies, and one magnifying filter.

IMP Optical Characteristics

Resolution	0.981 mrad/pixel (left); 0.985 mrad/pixel (right)
Focal length	23 mm
f/number	f/18
FOV	14.4° x 14.0°
Depth of Field	best focus, 1.3 m; DOF, 0.5 m to infinity

Electronics

The IMP has three electronics boards, all of which are housed in the lander chassis, in order to keep them warm (above -50° Celcius). They are connected to the onboard computer via the VME bus link. The first board is a copy of the DISR power supply, which provides all the necessary voltages for the CCD system from the lander 28 V power bus.

The second board sends clock pulses to the CCD. The twelve bit ADC also receives the analog signals back from the pre-amp board and converts them to digital signals over a period of two seconds, to be stored in the frame buffer chip on the third board.

The frame buffer board is connected to the VME backplane and is controlled by a field programmable gate array functioning as a state machine for command decoding. This third board also phases the steps and drives the three motors.

Filters

Center wavelengths are shown for both the left and right eyes, and are measured in nanometers.

Bandwidths shown are likewise for both left and right eyes, and are also measured in nanometers.

Responsivity (R) as a function of temperature (T) is shown for each filter and each eye as the parameters of a quadratic, where:

$$R(T) = a1 + (a2 * T) + (a3 * T^2)$$

Filter 0						
Filter Name	L440_R440					
Filter Application	Stereo, Geology					
Filter Type	Interference					
Center Wavelength (nm)	Left: 443.3		Right: 443.0			
Filter Bandwidth (nm)	Left: 26.2		Right: 26.2			
Responsivity, left eye	a1:	128.8	a2:	-0.387	a3:	-0.0007
Responsivity, right eye	a1:	117.9	a2:	-0.392	a3:	-0.0006

Filter 1						
Filter Name	L450_R670					
Filter Application	Solar					
Filter Type	Interference					
Center Wavelength (nm)	Left: 450.3		Right: 669.8			
Filter Bandwidth (nm)	Left: 4.91		Right: 5.30			
Responsivity, left eye	a1:	0.246	a2:	-0.0025	a3:	-0.00001
Responsivity, right eye	a1:	2.238	a2:	-0.0058	a3:	-0.00002

Filter 2	
Filter Name	L885_R947
Filter Application	Solar

Filter Type	Interference				
Center Wavelength (nm)	Left: 883.4		Right: 945.5		
Filter Bandwidth (nm)	Left: 5.60		Right: 43.7		
Responsivity, left eye	a1:	14.5	a2:	0.0233	a3: 0.00002
Responsivity, right eye	a1:	25.94	a2:	0.078	a3: 0.00005

Filter 3

Filter Name	L925_R935				
Filter Application	Solar				
Filter Type	Interference				
Center Wavelength (nm)	Left: 924.9		Right: 935.6		
Filter Bandwidth (nm)	Left: 5.03		Right: 4.91		
Responsivity, left eye	a1:	5.389	a2:	0.0193	a3: 0.00004
Responsivity, right eye	a1:	9.738	a2:	0.028	a3: -0.000003

Filter 4

Filter Name	L935_R990				
Filter Application	Solar				
Filter Type	Interference				
Center Wavelength (nm)	Left: 935.4		Right: 988.9		
Filter Bandwidth (nm)	Left: 4.84		Right: 5.39		
Responsivity, left eye	a1:	10.42	a2:	0.0378	a3: 0.00006
Responsivity, right eye	a1:	1.857	a2:	0.0064	a3: -0.000006

Filter 5

Filter Name	L670_R670				
Filter Application	Stereo, Geology				
Filter Type	Interference				
Center Wavelength (nm)	Left: 671.4		Right: 671.2		
Filter Bandwidth (nm)	Left: 19.7		Right: 19.5		
Responsivity, left eye	a1:	575.3	a2:	-0.570	a3: -0.0013
Responsivity, right eye	a1:	557.3	a2:	-0.575	a3: -0.0014

Filter 6

Filter Name	L800_R750
Filter Application	Geology
Filter Type	Interference

Center Wavelength (nm)	Left:	801.6	Right:	752.0		
Filter Bandwidth (nm)	Left:	21.0	Right:	18.9		
Responsivity, left eye	a1:	872.2	a2:	0.237	a3:	-0.0029
Responsivity, right eye	a1:	787.1	a2:	-0.247	a3:	-0.0019

Filter 7

Filter Name	L860_R-DIOPTER					
Filter Application	Geology					
Filter Type	Interference					
Center Wavelength (nm)	Left:	858.4	Right:	900.0		
Filter Bandwidth (nm)	Left:	34.4				
Responsivity, left eye	a1:	1435	a2:	2.491	a3:	0.0035
Responsivity, right eye	a1:	7596.9	a2:	9.057	a3:	-0.0235

Filter 8

Filter Name	L900_R600					
Filter Application	Geology					
Filter Type	Interference					
Center Wavelength (nm)	Left:	897.9	Right:	599.5		
Filter Bandwidth (nm)	Left:	40.8	Right:	21.0		
Responsivity, left eye	a1:	1120	a2:	3.006	a3:	0.0059
Responsivity, right eye	a1:	592.7	a2:	-0.598	a3:	-0.0013

Filter 9

Filter Name	L930_R530					
Filter Application	Stereo, Ranging, Geology					
Filter Type	Interference					
Center Wavelength (nm)	Left:	931.1	Right:	530.8		
Filter Bandwidth (nm)	Left:	27.0	Right:	29.6		
Responsivity, left eye	a1:	478.7	a2:	1.928	a3:	0.005
Responsivity, right eye	a1:	578.6	a2:	-0.893	a3:	-0.002

Filter 10

Filter Name	L1000_R480					
Filter Application	Geology					
Filter Type	Interference					
Center Wavelength (nm)	Left:	1002.9	Right:	479.9		

Filter Bandwidth (nm)	Left: 29.1		Right: 27.0		
Responsivity, left eye	a1:	213.4	a2:	1.606	a3: 0.0052
Responsivity, right eye	a1:	368.1	a2:	-0.668	a3: -0.002

Filter 11

Filter Name	L965_R965				
Filter Application	Stereo, Ranging, Geology				
Filter Type	Interference				
Center Wavelength (nm)	Left: 968.0		Right: 966.8		
Filter Bandwidth (nm)	Left: 31.4		Right: 29.6		
Responsivity, left eye	a1:	395.8	a2:	2.027	a3: 0.0051
Responsivity, right eye	a1:	393.5	a2:	2.185	a3: 0.0065

Operational Modes

Many optional command parameters are available to control the exposure and processing. These include everything from exposure time to the amount and type of data compression. Subframing boundaries and pixel averaging parameters can also be specified. All of this information is attached to the image headers.

Both lossless and lossy data compression are available. The lossless compression (with a compression rate between 1.3:1 and 2:1, depending on the busyness of the scene) employs a Rice algorithm developed at JPL. For cases where lossy compression is acceptable, compression rates between 6:1 and 24:1 can be obtained using a modified JPEG compressor, which uses arithmetic coding developed at the Technical University of Braunschweig. This compression is enhanced by local cosine transform prior to the JPEG-specific discrete cosine transform and made robust against data dropouts. Higher compression ratios are achieved using pixel blocking.

Additional alternatives for reducing the amount of data include image subframing and row and column averaging. Subframing is primarily useful when imaging targets like the Sun; most Sun images are returned as 31 x 31 pixel blocks. Row and column averaging can be used for sky images, providing a gradient and the edges of cloud features but not the high-resolution of a normal image.

For more details on IMP data compression, please see the IMP EDR archive dataset object or (Rueffer, 1995).

Calibration

The preparation of the IMP calibration files and algorithms has not yet been completed. Until it is, please see (Crowe, 1997) and Wellman, 1996)

Operational Considerations

There is some uncertainty in the height of the IMP camera above the surface of Mars. If we assume a relatively flat surface under the lander, then the height (h) of the elevation axis of the camera above the Martian surface is given by:

```
h = MAST + BASE + ISA + AIRBAG LAYER
```

where

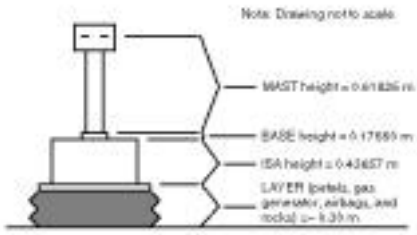

MAST	=	the distance between the stowed IMP elevation axis and the deployed IMP elevation axis (0.61825 m)
BASE	=	height of the stowed IMP elevation axis above the Integrated Support Assembly (ISA) (0.17550 m)
ISA	=	height of the ISA box (0.436576 m)
LAYER	=	the vertical distance between the local Martian surface and the bottom of the ISA box: includes the petal, the airbag gas generator, the airbags, rocks, and anything else between the ISA and the flat Martian surface. Current best estimate is 0.30 m +/- 50% uncertainty.

(Minor note: The optical axis is displaced ~0.012 m above the elevation axis.)

Therefore, the height of the camera in the stowed and deployed positions is:

```
STOWED_HEIGHT_ABOVE_SURFACE = 0.62 + ~ 0.30 = ~ 0.92 m
DEPLOYED_HEIGHT_ABOVE_SURFACE = 1.24 + ~ 0.30 = ~ 1.54 m
```

Given a roughly 50% uncertainty in the thickness of the AIRBAG LAYER, the uncertainty in the stowed and deployed heights of the camera are around 20% and 10%, respectively.

The flight model IMP has some measured characteristics which differ from the ideal, but which do not prevent success of the goals for mission science. These characteristics are:

1. Unequal toe-in between the two eyes.
2. Some vignetting is present, primarily about three image lines in the left eye due to the left mirror mount.
3. The left eye points downward about 0.8 milliradians compared to the right eye.
4. The eyes have image scales differing by about 0.4%.
5. Aliasing is significant at all wavelengths.
6. Alignment changes by about 0.5 milliradian as a function of the filter selected.
7. Camera pointing can be inexact due to a backlash effect.

Related Information

The following links provide some additional information about topics related to the Mars Pathfinder mission. You must be connected to the Internet for most of these links to work, since they are located at the Central Node of the Planetary Data System.

Mission

Mars Pathfinder

Instrument Host

Mars Pathfinder Lander

Targets

PDS Welcome to the Planets: Mars
PDS High Level Catalog: Mars, Phobos, Deimos

References

Cook, R., P. Katemeyn, and C. Salvo, Mars Pathfinder Project Mission Plan, JPL Document 11355, PF-100-MP-02, 90 pp., 1995.

Crowe, D.G., P.H. Smith, J.D. Weinberg,N. Chabot, G. Hoppa, R. Tanner, R. Reid,K. Herkenhoff, C. Shinohara, D.T. Britt,M. Burkland, S. Hviid, H.P. Gunnlaugsson,W. Goetz, N. Thomas, R. Marcialis, T. Friedman,L. Doose, R. Reynolds, J. N. Head, J. Wellman,B. Bos, and J. Maki, Imager for Mars Pathfinder Calibration Report, Lunar and Planetary Laboratory, University of Arizona, April 11,1997.

Rueffer, P., F. Rabe, and F. Fliem, Enhancement of IMP Lossy Image Data Compression using LCT, Space and Earth Science Data Compression Workshop, JPL Publication 95-9, 1995."

Smith, P.H., M.G. Tomasko, D. Britt, D.G. Crowe, R. Reid, H.U. Keller, N. Thomas, F. Gliem, P. Rueffer, R. Sullivan, R. Greeley, J.M. Knudsen, M.B. Madsen, H.P. Gunnlaugsson, S.F. Hviid, W. Goetz, L.A. Soderblom, L. Gaddis, and R. Kirk, The Imager for Mars Pathfinder Experiment, J. Geophys. Res., 102, 4003-4025, 1997.

Wellman, J.B., Calibration Report for IMP, JPL Document 13581, PF-4RSLIM01-01, March 29, 1996